

Composite Construction in Steel and Concrete IX

Proceedings of the Ninth International Conference on Composite Construction in Steel and Concrete



Edited by
Markus Knobloch,
Ulrike Kuhlmann,
Wolfgang Kurz, and
Markus Schäfer



Composite Construction in Steel and Concrete IX

Composite Construction in Steel and Concrete IX

Proceedings of the Ninth International Conference on
Composite Construction in Steel and Concrete
27–29th July 2021

Edited by
Markus Knobloch,
Ulrike Kuhlmann,
Wolfgang Kurz, and
Markus Schäfer

Editors:

Prof. Dr. sc. techn. habil. Markus Knobloch
Ruhr-Universität Bochum RUB
Germany

Prof. Dr.-Ing. Ulrike Kuhlmann
University of Stuttgart
Germany

Prof. Dr.-Ing. Wolfgang Kurz
Rheinland-Pfälzische Technische Universität
RPTU Kaiserslautern-Landau
Germany

Prof. Dr.-Ing. Markus Schäfer
University of Luxembourg
Luxembourg

Cover: Sankt Kilian Viaduct, Thuringia, Germany

Photograph: Institute of Structural Design,
University of Stuttgart

Note: The conference papers were first published online
in the journal *ce/papers – Proceedings in civil engineer-*
ing: <https://doi.org/10.1002/cepa.v6.1>

All books published by **Ernst & Sohn** are carefully produced. Nevertheless, authors, editors, and publisher do not warrant the information contained in these books, including this book, to be free of errors. Readers are advised to keep in mind that statements, data, illustrations, procedural details or other items may inadvertently be inaccurate.

Library of Congress Card No.: applied for

British Library Cataloguing-in-Publication Data
A catalogue record for this book is available from the British Library.

Bibliographic information published by the Deutsche Nationalbibliothek
The Deutsche Nationalbibliothek lists this publication in the Deutsche Nationalbibliografie; detailed bibliographic data are available on the Internet at <http://dnb.d-nb.de>.

© 2024 Ernst & Sohn GmbH, Rotherstraße 21,
10245 Berlin, Germany

All rights reserved (including those of translation into other languages). No part of this book may be reproduced in any form – by photoprinting, microfilm, or any other means – nor transmitted or translated into a machine language without written permission from the publishers. Registered names, trademarks, etc. used in this book, even when not specifically marked as such, are not to be considered unprotected by law.

Print ISBN: 978-3-433-03378-4
ePDF ISBN: 978-3-433-61191-3

Layout: Petra Franke, Ernst & Sohn GmbH
Printing: Media-Print GmbH

Printed on acid-free paper.

Preface	IX	<i>Kevin Wolters, Georgios Christou, Markus Feldmann</i>	
Composite Construction in Steel and Concrete	X	Probabilistic design of composite girders considering the degradation of the shear connection and the redistribution of forces	99
CODIFICATION	1		
<i>Nicole Schmeckebier, Wolfgang Kurz</i>		<i>Trent Phillips, Gian Andrea Rassati, James Swanson, Nadia Baldassino, Riccardo Zandonini</i>	
Engineering model for the vertical shear capacity of composite slabs with additional reinforcing steel	3	Progressive collapse modeling of a steel structure with composite slab using commercial finite element software	111
<i>Stephen Hicks, Markus Schäfer, Graham Couchman</i>			
European code developments	15	COMPOSITE BRIDGES	123
<i>Roberto T. Leon</i>		<i>Wojciech Lorenc, Günter Seidl, Robert Kühne</i>	
Evolution of USA composite codes: Changes in chapter I (composite construction) of the AISC 360-22	27	Composite dowels for bridges: trends and challenges for new European design rules	125
<i>Stephen Hicks, Matthias Braun, Zlatko Markovic, James Way</i>		<i>Richard Stroetmann, Cäcilia Karge, Tobias Mansperger</i>	
New Eurocode 4 design rules for composite beams with precast concrete slabs	40	Development of an orthotropic composite slab system for road bridges	139
<i>Ioan Diacu</i>		<i>Luís Vieira, José Oliveira Pedro, Rodrigo Gonçalves, Dinar Camotim</i>	
Potentially unsafe structural consequences in the design of composite beams shear connectors (a look at some of the Eurocode 4-1-1 design backgrounds)	50	Effect of cross-section bracing in steel-concrete composite bridge decks using the generalized beam theory	149
COMPOSITE BEAMS	61	<i>Mike Tibolt, Dennis Rademacher, Oliver Hechler, Kevin Wolters, Nils Rittich, Stoyan Ivanov</i>	
<i>Roland Bärtschi, Samuel Garcia, Robert Kroyer, Pascal Sutter</i>		Integral sheet piling abutments of modular composite bridges for a time efficient construction	161
Deformation capacity and ductility of shear connectors	63	<i>Radosław Sęk, Bogusław Pilujski, Dariusz Sobala, Wojciech Lorenc</i>	
<i>Samiran Adhikari, Gian Andrea Rassati, James A. Swanson, Rachel A. Chicchi</i>		New type of composite arch element using composite dowels: application in railway network arch bridge	173
High-definition modelling of composite beams	75	<i>Piotr Koziół, Wojciech Lorenc, Maciej Kozuch, Witold Kosecki, Adam Stempniewicz</i>	
<i>Philipp Hauser, Wolfgang Kurz</i>		New type of transition zone for steel-concrete hybrid beams in bridges	182
Non-linear analysis of composite beams with minimal modelling and calculation effort for strain-limited design	87		

CONTENTS

<i>Riccardo Zanon</i> Use of high-strength steel for slender medium span bridges: two recent case studies in France	192	<i>Qingjie Zhang, Markus Schäfer</i> Innovative numerical approaches for strain limited design of composite beams	295
COMPOSITE COLUMNS	205	<i>Joshua Henneberg, Peter Schaumann</i> Numerical analysis of early age movement in grouted connections	307
<i>Markus Schäfer, Qingjie Zhang, Pellumb Zogu, Marco Bergmann, Ozgun Ergun</i> Assessment of general method for composite column design in EN 1994-1-1 and comparison with simplified method	207	<i>Sina Kazemzadeh Azad, Brian Uy, Yifan Zhou, Yuchen Song, Jia Wang</i> Performance and design of stainless-steel composite structures – beams, columns and joints	320
<i>Ozgun Ergun, Markus Schäfer</i> Comparison of geometrical imperfection definitions on encased composite columns	219	FATIGUE AND FRACTURE	333
<i>Przemyslaw Schurgacz, Martin Neuenschwander, Markus Knobloch</i> Slender column strength of innovative concrete filled steel tube columns with high-performance building materials	231	<i>Lena Stempniewski, Ulrike Kuhlmann</i> Composite bridges with cracked concrete deck spanning between transverse beams under fatigue shear loading	335
<i>Mark Denavit</i> Variable stiffness reduction factor for stability design of steel-concrete composite columns	243	<i>Maryam Hosseini, Olivia Mirza, Fidelis Mashiri</i> Fatigue analysis of composite beam with bolted shear connectors	347
COMPOSITE DECKS	255	<i>Martin Mensinger, Florian Oberhaidinger, Lukas Stimmelmayer</i> Influence of hot dip galvanizing on the fatigue behaviour of T-studs for a grouted joint of integral composite frame bridges	354
<i>Valentino Vigneri, Christoph Odenbreit, Markus Schäfer, Stephen Hicks, Dennis Lam, François Hanus</i> Characterization of the load-slip behaviour of headed stud shear connections in narrow profiled sheeting	257	<i>Josef Karl Kraus, Karsten Geißler</i> Studies of the fatigue stress and strength of large composite bridges with cantilevers and precast concrete elements	364
<i>Leopold Sokol, Anna Palisson</i> Sagging bending resistance of composite slabs in partial shear connection	270	FIRE BEHAVIOUR	373
COMPOSITE STRUCTURAL ELEMENTS	281	<i>Manuel Romero, Vicente Alberó, Ana Espinos, Enrique Serra, Antonio Hospitaler, David Pons</i> A novel strategy for slim-floor fire protection	375
<i>Dongxu Li, Brian Uy, Zhichao Huang, Mahub Khan</i> Behaviour and design of high-performance steel and steel-concrete composite structures	283		

<i>Pascal Lequime</i> Advanced numerical fire design of industrial composite slabs with unprotected steel beams – a case study	384	<i>Riccardo Zanon, Dennis Rademacher, Günter Seidl, Daniel Pak</i> Integral bridge with RS-Overpass technology – step into the future standard highway overpasses	485
<i>Hitesh Lakhani, Jan Hofmann</i> Concrete cone failure of post installed fasteners during fire	396	JOINTS	497
<i>Oliver Beckmann, Michael Cyllok</i> Load transfer from hollowcore slabs to DELTABEAM® slim-floor beams in case of a Fire	404	<i>Nilde Maci, Jan Hofmann</i> Influence on the load-displacement behaviour of steel-to-concrete connections with post-installed adhesive anchors	499
<i>Alexey Tretyakov, Ilia Tkalenko, Kamila Cábová, František Wald</i> Finite element analyses for European model of the steel and fibre reinforced concrete circular hollow section column in fire	416	<i>Petr Cervenka, Jakub Dolejš</i> Steel FRC slab in compression in steel-concrete composite frame joints	510
<i>Takeo Hirashima, Fuminobu Ozaki, Tor Yoshida, Kei Kimura, Junichi Suzuki</i> Membrane action of reinforced concrete slabs in fire	422	<i>Michael Petrasch, Jan Hofmann</i> Strengthening of anchor channels on the concrete surface	522
<i>Kei Kimura, T. Hirashima, F. Ozaki, Tor Yoshida, Junichi Suzuki</i> Numerical analysis of load-bearing fire test for reinforced concrete slabs	434	<i>Maximilian Ziwes, Jakob Ruopp, Ulrike Kuhlmann</i> Studies on steel-to-concrete joints with concentrated loading conditions	534
INNOVATIVE STRUCTURES	447	PRACTICAL APPLICATIONS	547
<i>Hau Tran, Huu-Tai Thai, Brian Uy, Tuan Ngo, Dongxu Li, Jun Mo</i> Advanced analysis of steel-concrete composite buildings	449	<i>Maciej Kożuch, Wojciech Lorenc, Błażej Bartoszek, Adam Stempniewicz, Henryk Windorpski, Michał Struczyński, Radosław Sęk, Wojciech Ochojski</i> Application of rolled sections in composite bridges with span over 50 m	549
<i>Jovan Fodor, Markus Schäfer</i> Experimental and numerical investigation of the friction based demountable shear connector	461	<i>Ulrich Breuninger, Jonas Landsberger</i> Design, calculation and construction work of a prestressed composite construction to support the facade columns of a high-rise building	561
<i>Huu-Tai Thai</i> Innovative composite structural systems for modular tall buildings	473	<i>Xuemei Li, Ashpica Chhabra, Han Ding</i> Kunming Tower: composite systems in supertall design	573

CONTENTS

<i>Stefano China, Aroldo Tegon</i> NPS composite beams and columns used for the Odense university hospital	585	<i>Raul Avellaneda Ramirez, Matthew Eatherton, W. Samuel Easterling, Benjamin Schafer, Jerome Hajjar</i> Strength of concrete filled steel deck composite diaphragms with reinforcing steel	668
SEISMIC BEHAVIOUR	597	SHEAR CONNECTIONS	679
<i>Nicholas E. Briggs, Raul E. Avellaneda- Ramirez, Kyle Coleman, Benjamin W. Schafer, Matthew R. Eatherton, W. Samuel Easterling, Jerome Hajjar</i> Cyclic behavior of composite connections in compo- site floor diaphragms	599	<i>Taygun Yolacan, Markus Schäfer</i> Determination of slip-factor between friction shims and shot-blasted steel surfaces	681
<i>Yuko Shimada</i> Evaluation of the plastic deformation capacity of composite beams through the connection coefficient	611	<i>Yannick Broschart, Wolfgang Kurz, Kevin Wolters, Georgios Christou, Markus Feldmann, Josef Hegger, Martin Claßen</i> Development of a consistent design concept for composite dowels	693
<i>Yixin Zhang, Yang Liu, Jie Ruan, Pinzhi Wang</i> Seismic performance of prefabricated core steel tube reinforced concrete columns	621	<i>Cäcilia Karge, Richard Stroetmann, Joachim Wisniewski</i> Experimental and numerical investigation of dowel strips for longitudinal and transverse loading	705
<i>J. Ann Albright, Alessio Argentoni, Paolo M. Calvi</i> Experimental investigation of interior and exterior steel-concrete composite NPS beam-column joints	632	<i>Valentino Vigneri, Robert Kroyer, Stefano China, Alessio Argentoni, Andreas Taras</i> Longitudinal shear transfer in composite steel truss and concrete (CSTC) beams	717
<i>Luis B. Fargier-Gabaldon, Paul Cordova, Gustavo Parra-Montesinos, Gregory Deierlein</i> RCS moment frames in high seismic zones in the United States	644	<i>Angeliki Christoforidou, Florentia Kavoura, Marko Pavlovic, Milan Veljkovic</i> Mechanical performance of injected steel-reinforced resin connectors under different confined conditions for reusable composite structures	729
<i>Rafaela Don, Adrian Ciutina, Aurel Stratan, Cristian Vulcu</i> Slim-floor beam-to-column joints for seismic-resis- tant structures: joint performance and case study on MRFs	656		

Composite Construction is a key consideration in the design of buildings and infrastructure. Significant advances in research and development have increased the knowledge of the structural performance of composite structures. Some areas are becoming well understood and implemented in the design practice, codes and standards worldwide, while others like, e.g., application of high-performance materials or dismantlable and reusable composite members need further studies; trends that are reflected by the contribution to this conference. To make a full use of these innovations and advances, we need a forum for researchers, practitioners, and engineers to share and discuss their research, practical experience and innovations related to composite constructions in steel and concrete with their peers in an open, international forum.

The highly successful International Conference series on Composite Construction in Steel and Concrete are considered a major forum for the exchange of knowledge among the peers of the global composite construction community. The events started in 1987 in Henniker, New Hampshire, USA followed by Potosi, Missouri, USA in 1992. The conference was once held in Europe, which was the 3rd Composite Construction 1996 in Irsee, Germany. This event was followed by an event in the amazing scenery in Banff, Canada in 2000 as well as in 2004 at the Kruger National Park, South Africa. The 6th event was held 2008 in Devil's Thumb Ranch, Colorado, USA, before visiting Palm Cove, Queensland, Australia in 2013 and Jackson, Wyoming, USA in 2017.

These proceedings summarize the state-of-the art in composite construction worldwide, as presented at the 9th International Conference on Composite Construction in Steel and Concrete hosted by the Ruhr-Universität Bochum RUB, University of Stuttgart, RPTU Kaiserslautern-Landau and University of Luxembourg between the 27th and 29th July 2021. As a result of the global COVID-19 coronavirus pandemic, it is the first Composite Construction Conference that was held completely online.

The papers contained in this volume were selected through a rigorous review process and cover a wide variety of topics, including composite beams, composite columns, composite decks, joints, shear connections, fire behavior, seismic behavior, fatigue and fracture, codification, composite bridges, innovative hybrid structures, numerical investigations and practical applications representing the work of authors from 18 different countries around the world. One of the principles of the conference series is that it should represent a forum where the latest research and case studies are presented. Papers were therefore submitted only a few months before the conference and have been adapted based on the outcome of the discussions during the conference before the final publication, which ensures that only the most current work is presented.

This conference was organized by the members of the Chair of Steel, Lightweight and Composite Structures, Ruhr-Universität Bochum RUB, the Institute of Structural Design, University of Stuttgart, the Institute of Steel Structures, RPTU Kaiserslautern-Landau as well as the teaching and research area for Structural Engineering and Composite Structures, University of Luxembourg with the help, support and cooperation of the members of the International Scientific Committee, in particular the support of Professors W. Samuel Easterling, Jerome F. Hajjar, Roberto Leon, and Gian Andrea Rassati. We thank all expert reviewers for the time and effort they spent on the task of selecting and reviewing the papers. Our sincere thanks to all authors; the quality of this book is just the corollary of the high standard of their contributions, R&D activity and practical applications. Finally, we would like to acknowledge the effort and support provided by the partners and sponsors of the conference as well as the staff of our universities.

Markus Knobloch, Ulrike Kuhlmann,
Wolfgang Kurz and Markus Schäfer
February 2023

Composite Construction in Steel and Concrete IX

Proceedings of the Ninth International Conference on Composite Construction in Steel and Concrete,
July 27–29, 2021

About this conference

The highly successful International Conference series on Composite Construction in Steel and Concrete is a major forum for researchers, practitioners, and engineers to share and discuss their research, practical experience and innovations related to composite constructions in steel and concrete with their peers of the global composite construction community. One of the principles of the conference series is that it should represent a forum where the latest research and case studies are presented. Papers are therefore submitted only a few months before the conference and may be adapted based on the outcome of the discussions during the conference, which ensures that only the most current work is published. The CCIX was hosted by the Ruhr-Universität Bochum RUB, University of Stuttgart, RPTU Kaiserslautern-Landau and University of Luxembourg in July 2021. As a result of the global COVID-19 coronavirus pandemic, it is the first Composite Construction Conference to be held completely online.

Review Process

All papers published in this issue were peer-reviewed by the Scientific Board of the conference series.

Committees:

Local Organizing Committee

Ulrike Kuhlmann	University of Stuttgart	Germany
Markus Knobloch	Ruhr-Universität Bochum RUB	Germany
Wolfgang Kurz	RPTU Kaiserslautern-Landau	Germany
Markus Schäfer	Universität Luxembourg	Luxembourg

Scientific Committee

Roland Bärtschi	Bärtschi Ingenieure	Switzerland
Alain Bureau	Centre Technique De La Construction Metallique (CTICM)	France
Adrian Ciutina	Polytechnic University of Timisoara	Romania
Graham Couchman	Steel Construction Institute (SCI)	UK
W. Samuel Easterling	Iowa State University	USA
Jerome Hajjar	Northeastern University	USA
Stephen Hicks	University of Warwick	UK
Markus Knobloch	Ruhr-Universität Bochum RUB	Germany
Venkatsh Kodur	Michigan State University	USA
Ulrike Kuhlmann	University of Stuttgart	Germany
Wolfgang Kurz	RPTU Kaiserslautern-Landau	Germany
Dennis Lam	University of Bradford	UK
Jean-Paul Lebet	École Polytechnique Fédérale de Lausanne	Switzerland
Roberto Leon	Virginia Polytechnic Institute and State University	USA
Matti V. Leskela	University of Oulu	Finland
Richard Liew Jat Yuen	National University of Singapore	Singapore
Renata Obiala	ArcelorMittal Global R&D	Luxembourg
José Oliveira Pedro	Instituto Superior Técnico de Lisbon	Portugal
Gian Andrea Rassati	University of Cincinnati	USA
Manuel L. Romero	Universitat Politècnica de València	Spain
Markus Schäfer	Universität Luxembourg	Luxembourg
Brian Uy	University of Sydney	Australia
Milan Veljkovic	Delft University of Technology	Netherlands
František Wald	Czech Technical University in Prague	Czech Republik
Rebekka Winkler	Ruhr-Universität Bochum RUB	Germany
Ben Young	The Hong Kong Polytechnic University	China

Organized by



Ruhr-Universität
Bochum RUB



RPTU
Kaiserslautern-Landau



University of Stuttgart

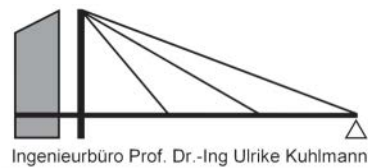


Université du
Luxembourg

Partners



Sponsors



Support



CODIFICATION

ENGINEERING MODEL FOR THE VERTICAL SHEAR CAPACITY OF COMPOSITE SLABS WITH ADDITIONAL REINFORCING STEEL

Nicole Schmecke**bier***, Wolfgang Kurz******

* KREBS+KIEFER Ingenieure GmbH Köln
e-mail: schmecke**bier.nicole@kuk.de**

** Technische Universität Kaiserslautern
e-mail: wolfgang.kurz**@bauing.uni-kl.de**

Keywords: Composite Slabs, Shear Capacity, Engineering Model, Design, Standards, Experimental Investigations.

Abstract. *Up to now, no independent model for the shear design of composite slabs under the consideration of the two types of longitudinal reinforcement – metal sheet and reinforcing steel – exists. Therefore, extensive investigations were conducted at Technische Universität Kaiserslautern. The research project was completed recently. A new engineering model, which was calibrated on tests, was developed. Furthermore, the engineering model was transferred into a design model. In this paper the experimental investigations are presented as well as the engineering model.*

1 INTRODUCTION

Eurocode 4 [1] says that the shear capacity of composite slabs should be calculated according to Eurocode 2 [2] by using the empirical supported formula of concrete slabs without shear reinforcement. This formula refers on the one hand to the tooth model from Reineck [3] and on the other hand to the analysis of an extensive data base of shear tests on concrete specimen [4]. This model is based on some assumptions that are not valid for composite slabs. The metal sheet has its own shear capacity and the dowel effect of the slab is weaker than the dowel effect of the reinforcing steel. Furthermore, the bond stiffness of metal sheets is significantly lower than that of reinforcing steel. In addition, there is the fact that the empirical formula of Eurocode 2 [2] was determined by analysis of an extensive database of shear tests only on concrete specimen.

Furthermore, a lack of security for the calculation of the shear capacity of composite slabs made of lightweight concrete was noticed in [5]. In this paper tests on composite slabs are described, whereby the aim of this research was the investigation of the longitudinal bond action. The observed failure mode was a combination of longitudinal shear and transverse shear failure. Therefore, a new design model for the shear capacity of composite slabs without additional reinforcement [6] was developed at Technische Universität Kaiserslautern. This design model is valid for composite slabs made of lightweight concrete as well as normal concrete, but the main focus of this research project were the studies on specimens with lightweight concrete. The model contains three mechanisms that act additive. The shear capacity of the metal sheet and the bearing capacity of the uncracked compression zone together are described as the basic value because they act permanently. A third mechanism, the tensile bearing effects in the crack tip, can be added for re-entrant profiles. This shape guarantees an effective bond action so that critical crack width can be avoided.

In practice, composite slabs are mostly built with additionally reinforcement. But the significant influence of the reinforcing steel cannot be considered entirely in the model of [6]. Therefore, further research was necessary.

2 EXPERIMENTAL INVESTIGATIONS

2.1 General

In general, shear failure doesn't occur in composite slabs. So, the enforcement of shear failure in tests is very difficult. Therefore, the specimens were designed as small stripes of slabs and with uncommon dimensions. Two cross sections are shown as an example in figure 1. To avoid longitudinal shear failure an effective end anchorage was used. As reinforcing steel threaded anchor bars made of high strength steel [7] with a diameter of 15 mm were used to increase the bending capacity compared to the shear capacity disproportionately. In accordance with the rules, the reinforcing steel was placed as mesh reinforcement directly on the top of the metal sheet. In each rib one rebar was located and normal concrete C30/37 was used. The test setup was realised as a three-point-bending-test with an offset arrangement of the load. The distance between the support and the load introduction was set to three times of the effective height d_m . The width of the specimens corresponded to twice of the ribs of the metal sheet.

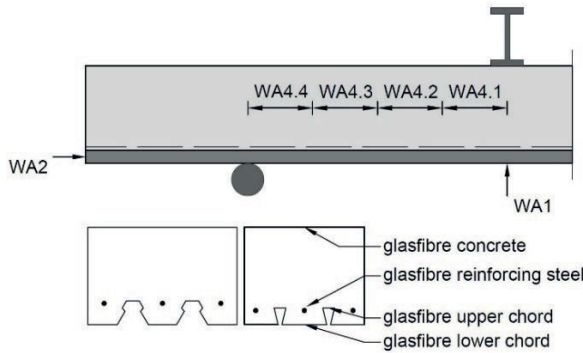


Figure 1. Schematic representation of cross sections of specimens and arrangement of measurement.

Table 1: Overview of combination of parameters of tests and failure loads of tests.

combination	metal sheet	thickness of metal sheet	height	width	f_{ctm}	f_{cm}	reinforcement	V_{test}
[-]	[-]	[mm]	[mm]	[mm]	[N/mm ²]	[N/mm ²]	[-]	[kN]
1	SHR [8]	1.00	300	370	2.1	24.4	Ø15/15	168.0 137.2
2	C70 [9]	1.00	300	460	2.1	24.4	Ø15/18	172.2 185.6
3	Hody [10]	1.00	280	500	2.0	24.9	Ø15/20	178.9 164.0
4	ComFlor 80	1.00	280	690	2.0	24.9	Ø15/30	248.9 249.6
5	Hody [10]	0.75	280	500	2.4	27.8	Ø15/20	209.4 180.3
6	SHR [8]	0.75	300	370	2.4	27.8	Ø15/15	139.9 157.3
7	SHR [8]	1.25	300	370	2.4	27.8	Ø15/15	151.4 181.3
8	SHR [8]	1.00	300	370	2.2	25.0	Ø20/15	144.7 -
9	Hody [10]	1.00	280	500	2.2	25.0	Ø20/20	225.2 215.8
10	SHR [8]	1.00	300	370	3.3	56.1	Ø15/15	224.2 226.8
11	Hody [10]	1.00	280	500	3.3	56.1	Ø15/20	259.3 -
12	C70 [9]	1.00	300	460	2.6	31.0	Ø15/18 u	- 190.7
13	ComFlor 80	1.00	280	690	2.6	31.0	Ø15/30 u	270.4 244.0
14	SHR [8]	0.75	250	370	2.5	30.4	Ø15/15	168.7 120.3
15	C70 [9]	1.00	250	460	2.5	30.4	Ø15/18	146.2 163.1

u \triangleq location of reinforcing steel in through with $c_{nom} = 20$ mm, - \triangleq outlier

Four different metal sheets were tested, whereby re-entrant profiles were included as well as profiles with an open shape. Furthermore, parameters were varied specifically to investigate their influence on the bearing behaviour. The parameters are the thickness of the metal sheet, the ratio of longitudinal reinforcement, the concrete strength, the location of the reinforcing steel and the height of the slab. Table 1 gives an overview over the combinations of the parameters. Two tests were performed with each combination. The specimens were named using the following principle: shape of metal sheet – thickness of metal sheet – height of specimen – concrete compressive strength – additional longitudinal reinforcement.

2.2 Test Results

The shear failure of composite slabs with additional reinforcing steel is very different to the bearing behaviour according to shear of concrete slabs. To explain that, the observations during the test procedure are described on the example of test C70-1,00-300-C30/37-Ø15/18h-1. Therefore, the force-deflection-diagram is shown in figure 2 and in figure 3 different crack patterns are presented. At a shear force of 30 kN the first bending cracks occurred, which results in the first change of the stiffness in the force-deflection-curve. With increasing load further formation of bending cracks could be observed. At a shear force of about 110 kN the diagram shows a significant load drop, which is followed by the second change of stiffness. The picture in the middle of figure 3 shows that a new crack appeared. This crack reaches the uncracked compression zone and runs inclined, so it could be identified as the shear crack. Because the shear crack wasn't critical, the cylinder load could be increased. During the load increase the crack propagation was still stable and a third area with a constant gradient could be seen in the force-deflection-diagram. The last picture in figure 3 shows that the further crack development was concentrated near to the support, because it was the horizontal part of the shear crack. At a shear force of about 160 kN the deflection of the specimen increased and the failure occurred a short time later. The failure was characterised by the opening of the shear crack. In summary the force-deflection-curve could be divided into four areas. The first one is the uncracked condition, followed by the area characterised by the formation of bending cracks. The third area describes the formation of the horizontal part of the shear crack and the last area is the failure of the specimen. Compared to concrete specimens which fail suddenly the behaviour at failure is different. After the shear crack reaches the concrete compression zone, the crack formation is still stable and the load could be increased significantly.

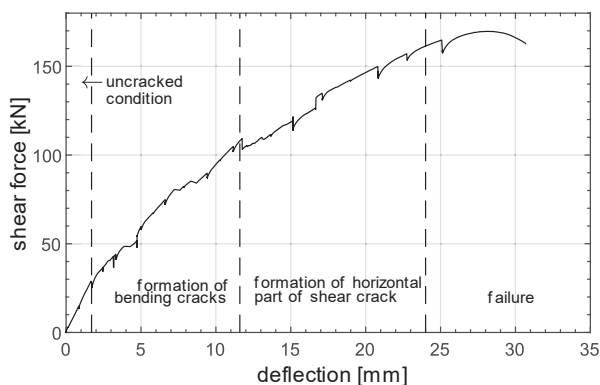


Figure 2. Force-deflection-diagram of test C70-1,00-300-C30/37-Ø15/18h-1.

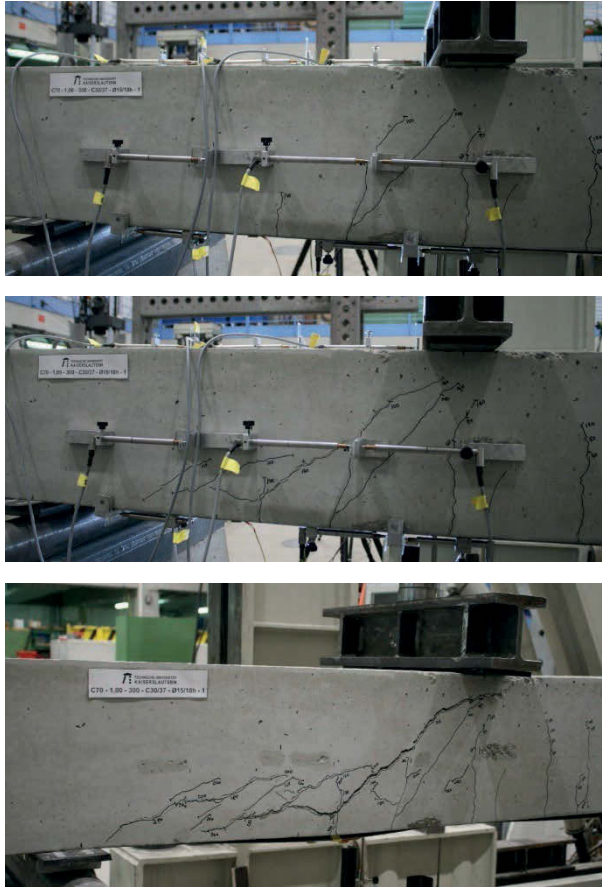


Figure 3. Crack patterns of test C70-1,00-300-C30/37-Ø15/18h-1
top: $F_{cyl} = 140$ kN, middle: $F_{cyl} = 160$ kN, bottom: Fracture pattern.

To investigate the crack pattern inside the specimens some selected ones were sliced. As an example, a picture of the longitudinal cut through the upper chord of the metal sheet of test C70-1,00-300-C30/37-Ø15/18h-1 is shown in figure 4. First of all, it is obvious that the crack pattern inside and outside the specimen differs. Only one crack is visible. It runs horizontal on the location of the smallest concrete width to the support. This observation was confirmed by the other sliced specimen. The oblique cracks on the outside of the specimen are the result of marginal influences.



Figure 4. Longitudinal cut through the upper chord of specimen C70-1,00-300-C30/37-Ø15/18h-1.

The strains of the metal sheets were continuously measured with glass fibre cables on the upper chord as well as on the lower chord. Thus, it could be determined, that at the location of the shear crack the strains of the lower chord reached their maximum where the strains on the upper chord reached their minimum. Contrary to the expectation the maximum strains in the metal sheet are not at the location of the maximum bending moment of the specimen. Furthermore, the concrete compressive strains on the top of the specimen were measured. Following the Bernoulli Hypothesis, the concrete strains should increase constantly from the support to the load introduction. On the contrary a steady increase could only be observed at the location of the shear crack. Then, the concrete compressive strains increased significantly with their maximum at the load introduction. These observations lead to the conclusion that the Bernoulli Hypothesis is not valid for the shear force bearing behaviour of composite slabs. When the shear crack occurs, the bearing behaviour changes to a tied arch model with two compression struts. The concrete in the location of the shear crack supports itself on the metal sheet, which results in the high measured strains. The second compression strut runs directly to the support.

3 NEW ENGINEERING MODEL

3.1 Basic description of the design model

From the observations in the tests and the continuous strain measurement by glasfibres a simplified truss model was developed. It is presented in figure 5. After the shear crack occurs the concrete supports itself on the metal sheet which transfers the shear force through the crack. Then, the dowel effect of the longitudinal reinforcement induces the forces back into the concrete. This is characterised by the tension strut in the truss model that brings the forces of the direct compression strut into the support. The horizontal tie which is necessary for the equilibrium is the longitudinal reinforcement.

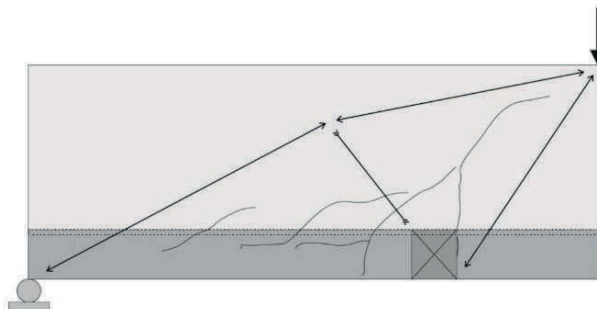


Figure 5. Truss model of shear transfer in composite slabs.

On the basis of the described truss model the engineering model for the design of the shear capacity of composite slabs with additional reinforcing steel was developed. The model is shown in figure 6 and contains four mechanisms that act additive. The shear transfer in the concrete compression zone $V_{c,cz}$, the shear transfer in the crack propagation zone $V_{c,et}$ and the shear capacity of the tension strut that fails by kinking of the reinforcement or spalling of the concrete in the ribs $V_{c,ks}$ establish the equilibrium in the shear crack. In addition the vertical component of a strut that transfers the load to the support $V_{c,cs}$ is considered. The failure occurs when one of the mechanisms fails. The failure of the dowel effect of the reinforcement was identified as the kinematic condition for the overall failure of the specimen. Due to that the opening of the shear crack was possible which leads into the loss of the tensile bearing effects in the crack tip. The remaining two mechanisms cannot compensate these forces.

The strain measurement in the tension area showed that the metal sheet always reached the maximum tension bearing capacity in section II-II. Therefore, it is proposed to allocate the fully anchored tensile force to the metal sheet following the partial bond theory. The rest of the tension force, which is necessary for

the equilibrium of moments, should be referred to the reinforcing steel. Furthermore, the high utilisation of the metal sheet is the reason that the own shear capacity of the metal sheet is not considered in the described model.

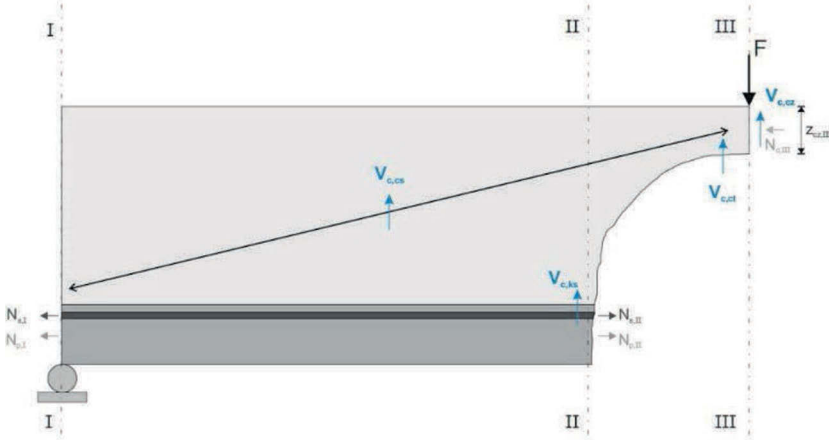


Figure 6. New shear design model for composite slabs with reinforcing steel.

3.2 Shear capacity of the uncracked compression zone $V_{c,cz}$

The shear capacity of the uncracked concrete compression zone $V_{c,cz}$ uses the height of the compression zone z_{pl} . This height depends on the tension forces in the steel sheet and the reinforcing steel in cross section II-II and the compression force in cross section III – III that represents the bending moment present in cross section III-III. The equation (1) was developed by Hartmeyer [6] with reference to Zink [11] and is assumed for this model. The factor $2/3$ represents a parabolic distribution of the shear stresses in the concrete compression zone. It has to be noted that the use of a constant stress distribution of the normal stresses in the compression zone (see equation (2)) in combination with the parabolic distribution of the shear stresses is not consistent from the mechanical point of view. The use of a linear distribution of the normal stresses, which would be mechanically correct, is uncommon for composite constructions. In the interest of the Ease of Use this discrepancy is accepted.

Because the strain measurement with glasfibers showed that compared to the reinforcing steel the strains in the metal sheet were significantly higher, it is suggested to use the full anchored normal force of the metal sheet. The remaining forces necessary for the realisation of the bending moment should be assigned to the reinforcing steel.

$$V_{c,cz} = \frac{2}{3} \cdot z_{pl,III} \cdot b \cdot f_{ctm} \quad (1)$$

$$z_{pl,III} = \frac{N_{s,II} + N_{p,II}}{b \cdot f_{cm}} \quad (2)$$

3.3 Shear capacity of crack propagation zone $V_{c,ct}$

Hillerborg [12] introduced the critical length as a factor to describe the crack length that is able to transfer tensile stresses perpendicular to the crack. Hartmeyer [6] and Zink [11] used this approach to determine the shear capacity depending on the fracture energy G_f of the concrete. In this model the approach from Hartmeyer [6] was used and enhanced, s. equation (3).

$$V_{c,ct} = \alpha \cdot \beta \cdot l_{ch} \cdot b \cdot \frac{d_s}{d_{s,0}} = 0,12 \cdot \frac{G_f \cdot E_{cm}}{f_{ctm}} \cdot b \cdot \frac{d_s}{d_{s,0}} \quad (3)$$

The fracture energy is determined by the rules of Model Code 2010 [13]. The factors, which are necessary for the description of the characteristic length, were assumed from Rimmel [14] and Grimm [15] ($\beta = 0,4$) and Reinhardt et al. [16] ($\alpha = 0,3$). The length of the shear crack with small crack width is not only dependent on the material behaviour but also on the total length of the crack. Good results were received by using the basic formula on very thick slabs. For the application in thinner slabs a linear dependence of the effective crack length on the effective height d was assumed. The basic value $d_{s,0}$ limits this effect to the maximum height d_s for which experimental data exists. The linear proportionality is a simplified assumption.

The investigation of the crack patterns in the test showed that the shear crack runs nearly horizontal when reaching the uncracked compression zone. Therefore, the consideration of the angle of the shear crack is not necessary.

3.4 Shear capacity inducing kinking and spalling $V_{c,ks}$

Two failure modes has to be considered, concrete failure $V_{c,ks,1}$ and steel failure $V_{c,ks,2}$, where the one with the lowest shear capacity should be used for the mechanism $V_{c,ks}$ according to equation (4).

$$V_{c,ks} = \min \left\{ V_{c,ks,1} \right. \\ \left. V_{c,ks,2} \right\} \quad (4)$$

For the shear capacity inducing spalling the approach from Baumann and Rüsç [17] was enhanced according to equation (5). In figure 4 a horizontal crack can be found. As explained this crack occurs in all test specimen and it is located at the minimum width between shear connectors in the webs of the steel sheets. The width $b_{min,bar}$ has to be taken as the minimum width described above minus the diameter of the longitudinal reinforcement. Baumann and Rüsç [17] introduced a length d_{eq} in their formula which was adapted here to the height h_{pc} . For all types of steel sheets with shear connectors in the webs the height of the lowest connector above the bottom chord of the sheet is taken as h_{pc} . It is assumed that in other cases with re-entrant profiles h_{pc} is the middle between the upper and lower chord which both introduce shear by contact forces perpendicular to the span. The geometry values b_{min} and h_{pc} are explained in figure 7. In [17] the third square root of the concrete compressive strength was used to take the concrete tensile strength into account. Equation (5) shows that the concrete tensile strength is here considered directly with f_{ctm} .

$$V_{c,ks,1} = 1,64 \cdot b_{min,bar} \cdot h_{pc} \cdot f_{ctm} \quad (5)$$

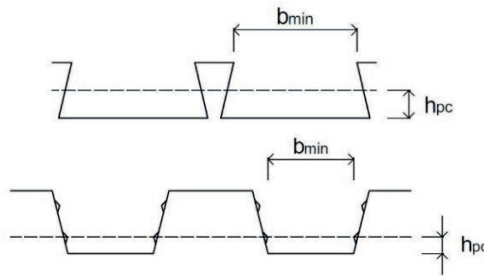


Figure 7. Geometry values b_{min} and h_{pc} .

The equations for the kinking resistance of the longitudinal reinforcement were taken from Model Code 2010 [13], see equation (6). Factor η_s is the utilization ratio of the reinforcing steel. As mentioned before, in all tests we observed that the utilization of the steel sheet was significantly higher than that of the reinforcement. Therefore, we propose that first the full utilization of the steel sheet in the decisive section

is assumed and then the remaining tensile force is used to determine the utilization of the reinforcement. Furthermore, the approach in [13] contains a formulation dependent on the displacement of the crack origins. With a displacement of $0,2 \cdot d_s$ the maximum dowel effect can be activated. This formulation represents a criterion of serviceability. Because on the one hand the design of the shear force bearing behaviour belongs to ULS and on the other hand in the tests crack displacements in the range of $0,2 \cdot d_s$ could be observed the expression depending on displacement could be neglected.

$$V_{c,ks,2} = 1,6 \cdot A_s \cdot \sqrt{f_{sk}} \cdot \sqrt{f_{cm}} \cdot \sqrt{1 - \eta_s^2} \quad (6)$$

3.5 Shear capacity of the direct compression strut $V_{c,cs}$

The vertical component of the direct compression strut is another component of the shear capacity of composite slab in those cases where a strut can directly anchor on a direct support. The direct compression strut is at equilibrium with the anchored tension force in section I-I, so the vertical component has to be calculated according equation (7). In correspondence to concrete members the inclination angle of the compression strut is named θ .

$$V_{c,cs} = (N_{s,I} + N_{p,I}) \cdot \tan \theta \quad (7)$$

In all test specimen the slabs were longer than the span so an overhanging length of about 500 mm was used to anchor the tension forces in the steel sheet and in the reinforcement. Due to the fact, that the bending moment at the support is about zero (just a small hogging moment out of dead weight of the slab) it is absolutely necessary that there has to be some bending moment in the concrete slab to reach this equilibrium. In some tests some minor cracks have been detected at to top side of the composite slab in the region of the support at ULS. Therefore, it is assumed as a simplification that the stresses in the concrete have a triangular shape with a concrete stress about zero at the top edge of the slab, see figure 8. This leads to the simplified assumption that the position of the direct compression strut is located at $1/3$ of the height of the slab. For rectangular members this approach is correct. But in composite slabs the concrete in the area of the metal sheet is constricted, which has to be considered by determining z_{SP} as position of the centroid of compression stresses.

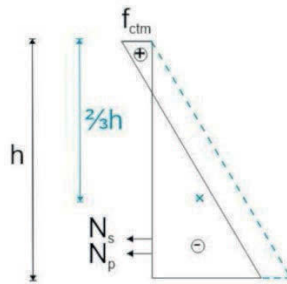


Figure 8. Stress distributions in concrete in section I-I.

At its opposite end the direct compression strut begins at the uncracked compression zone above the shear crack. In all test specimen this strut started at the load introduction into the specimen. So, the inclination angle could be determined according to equation (8), where z_{pl} has to be determined with the tension forces in section II – II of figure 6.

$$\tan \theta = \frac{z_{SP} - 0,5 \cdot z_{pl,III}}{3 \cdot d_m} \quad (8)$$

Because of the dependency of the shape of the metal sheet the calculation of $\tan \theta$ is time consuming. Therefore, a parameter study was done to provide a simplified assumption of $\tan \theta$. For the parameter study common cross sections of decks were used. The applied loads were chosen that high that the cross sections reached their bending capacity. Due to that the height of the uncracked compression zone increases and the inclination angle of the compression strut decreases. Figure 9 shows the results of the parameter study. For the simplified assumption of $\tan \theta$ the value 0.21 was chosen as the minimum value. In general, for thinner decks in combination with higher concrete compressive strength greater values could be observed. Because higher concrete compressive strength are rarely used in composite slabs and the use of formula (8) is time-consuming, $\tan \theta = 0.21$ is a satisfied assumption.

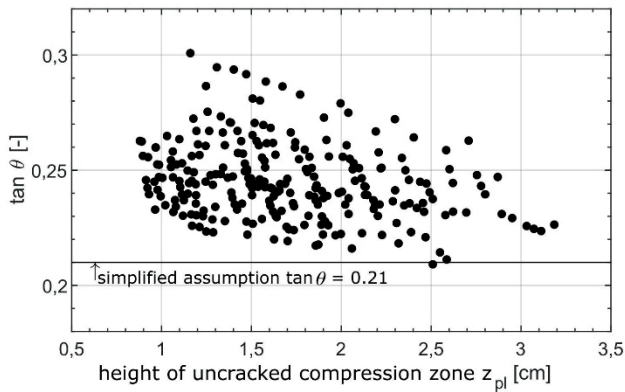


Figure 9. Results of parameter study to $\tan \theta$.

4 VERIFICATION AND STATISTICAL ANALYSIS OF THE DESIGN MODEL

With the developed model the shear force capacity could be calculated depending on the bending load. So, the model is very different to the current model [2] which describes the shear force capacity of a cross section of a bending member. Like described above three of the mechanisms are depending on the utilisation ratio of the longitudinal reinforcement. Thus, an independent consideration is not possible.

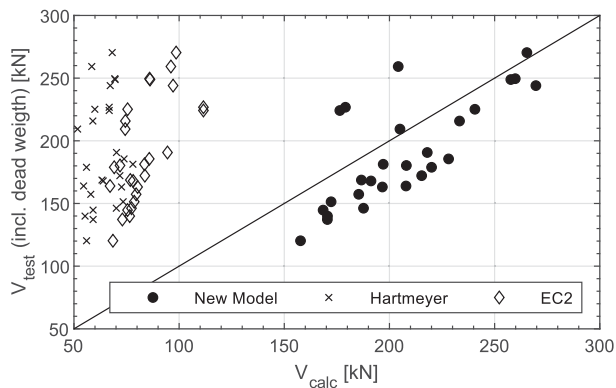


Figure 10. Comparative presentation of test results with calculated shear forces as mean values.

Figure 10 shows the plot of ultimate load in the tests V_{test} vs. the ultimate load according the developed design model V_{calc} . It shows a very good accordance between the tests and the model. Furthermore, the accordance is independent from the shape of the metal sheet. Also plotted in figure 10 are the comparisons between the test results and the shear forces calculated with the model of the current EN 1992 [2] and the model of Hartmeyer [6]. It becomes clear that with these models the shear force capacity of composite slabs cannot be described reliable. Even though the capacities are on the safe side, only with the new developed model the capacities can be calculated economical. Table 2 contains the values describing the mathematical reliability of the models. The new developed model is considered in the draft of Eurocode 4 [18].

Table 2: Comparison of test results with calculated shear forces as mean values.

Design Model	Mean Value	Standard deviation	Coefficient of determination
New Model	0,918	0,141	0,572
Eurocode 2 [2]	2,296	0,387	0,412
Hartmeyer [6]	3,001	0,676	0,031

The recalculation of the tests with the developed model was done at the location of the shear crack. Because the prediction of the location of the shear crack isn't possible at that time in practice the calculation of the shear force capacity has to be done in the given section in the distance d from the support. The model was statistical analysed and the mean values of the material strength were transferred into characteristic values. With a safety factor of $\gamma_R = 1,3$ the design value of the shear force capacity could be calculated according equation (9). The equations for the calculation of the mechanisms on the characteristic level are summarised in table 3.

$$V_{Rd} = \frac{0,694}{\gamma_R} \cdot [V_{c,cz} + V_{c,ct} + V_{c,ks} + V_{c,cs}] \quad (9)$$

Because with the developed model the calculation of the normal forces in different sections is necessary for the calculation of the shear force capacity the question arises whether the model could be simplified for the Ease of Use in practice. Therefore, a simplified design check is proposed. Only the tensile forces in the section of the support has to be calculated and used for the calculation of the different mechanisms. The tension force at support is at equilibrium with the compression force in the known distance d from the support. A verification of this approach was done with different statistical analysis. More information can be found in [19].

Table 3: Summary of equations for the calculation of the design shear force capacity.

Mechanism	Calculation
Compressive zone	$V_{c,cz} = \frac{2}{3} \cdot z_{pl} \cdot b \cdot f_{ctm}$ <p>with: $z_{pl} = \frac{N_{s,II} + 1,15 \cdot \tau_{rk} \cdot b \cdot L_{II}}{1,33 \cdot b \cdot f_{ck}}$</p> <p>$z_{pl}$ = height of uncracked compression zone f_{ctm} = mean value of cylinder tensile strength of concrete $N_{s,II}$ = normal force in reinforcing steel in section II-II τ_{rk} = characteristic value of longitudinal shear stress of metal sheet L_{II} = horizontal distance between section I-I and II-II f_{ck} = characteristic cylinder compressive strength of concrete</p>
Crack propagation zone	$V_{c,ct} = 0,12 \cdot \frac{G_f \cdot E_{cm}}{f_{ctm}} \cdot b \cdot \frac{d_s}{d_{s,0}}$ <p>with: $G_f = 73 \cdot f_{cm}^{0,18}$ fcm [N/mm²] G_f = fracture energy of concrete [N/m] E_{cm} = mean value of Young`s modulus d_s = effective height of reinforcing steel $d_{s,0}$ = basic value of effective height of reinforcing steel = 270 mm</p>
Dowel effect	$V_{c,ks} = \min\{V_{c,ks,1}; V_{c,ks,2}\}$ <p>with: $V_{c,ks,1} = 1,64 \cdot b_{min} \cdot h_{pc} \cdot f_{ctm}$</p> <p>$b_{min}$ = minimum width of concrete inside of the metal sheet h_{pc} = vertical distance between bottom edge of metal sheet and the lowest shear connector</p> $V_{c,ks,2} = 1,6 \cdot A_s \cdot \sqrt{f_{sk}} \cdot \sqrt{f_{ck}} \cdot \sqrt{1 - \eta_s^2}$ <p>A_s = cross section of reinforcing steel f_{sk} = characteristic value of yield strength of reinforcing steel η_s = utilisation ratio of reinforcing steel</p>
Direct compression strut	$V_{c,cs} = \tan \theta \cdot (N_{s,I} + N_{p,I})$ <p>with: $\tan \theta = \frac{z_{SP} - 0,5 \cdot z_{pl}}{3 \cdot d_m}$</p> <p>$N_{p,I} = 1,15 \cdot \tau_{rk} \cdot b \cdot L_I$ θ = inclination angle of compression strut $N_{s,I}$ = normal force of reinforcing steel in section I-I $N_{p,I}$ = normal force of metal sheet in section I-I z_{SP} = location of compression strut from the top edge of deck d_m = mean value of effective height L_I = bond length of metal sheet behind the support</p>

REFERENCES

- [1] DIN EN 1994-1-1 2010, *Eurocode 4: Bemessung und Konstruktion von Verbundtragwerken aus Stahl und Beton – Teil 1-1: Allgemeine Bemessungsregeln und Anwendungsregeln für den Hochbau, Deutsche Fassung EN 1994-1-1:2004 + AC:2009*, Beuth, Berlin.
- [2] DIN EN 1992-1-1 2010, *Eurocode 2: Bemessung und Konstruktion von Stahlbeton- und Spannbetontragwerken – Teil 1-1: Allgemeine Bemessungsregeln und Regeln für den Hochbau, Deutsche Fassung EN 1992-1-1:2004 + AC:2010*, Beuth, Berlin.
- [3] Reineck, K.-H., *Ein mechanisches Modell für den Querkraftbereich von Stahlbetonbauteilen*, Dissertation, Universität Stuttgart, 1990.
- [4] Reineck, K.-H., Kuchma, D.A. und Fitik, B., “Erweiterte Datenbanken zur Überprüfung der Querkraftbemessung für Konstruktionsbauteile mit und ohne Bügel”, *DAfStb-Heft 597*, 2012.
- [5] Brüdern, A.-E., Mechtcherine, V., Kurz, W. and Jurisch, F., “Self-Compacting Lightweight Aggregate Concrete for Composite Slabs”, *Proceedings of Advanced Concrete Materials International Conference*, Stellenbosch, South-Africa, 2009.
- [6] Hartmeyer, S., *Modell zur Beschreibung des Querkrafttragverhaltens von Stahlverbunddecken aus Leicht- und Normalbeton*, Dissertation, Technische Universität Kaiserslautern, 2014.
- [7] Z-12.5-96, *Allgemeine bauaufsichtliche Zulassung Z-12.5-96 – Ankerstabstahl St 900/1100 mit Geweinderippen AWM 1100 Nenn Durchmesser: 15 und 20 mm*, Stahlwerk Annahütte Max Aicher GmbH & Co. KG, 01.10.2015 – 01.10.2020, Berlin, 2015.
- [8] Z-26.1-45, *Allgemeine Bauartgenehmigung Z-26.1-45 – SUPER-HOLORIB SHR 51-Verbunddecke*, Montana Bausysteme AG, 13.03.2018 – 13.08.2023, Berlin, 2018.
- [9] Z-26.1-22, *Allgemeine bauaufsichtliche Zulassung Z-26.1-22 – COFRASTRA Verbunddecken*, ArcelorMittal Construction Deutschland GmbH, 28.07.2016 – 28.07.2021, Berlin, 2016.
- [10] Z-26.1-52, *Allgemeine Bauartgenehmigung Z-26.1-52 – Verbunddecke Hody SB 60, REPPEL b.v. Bouwspecialiteiten*, 01.07.2019 – 01.07.2024, Berlin, 2019.
- [11] Zink, M., *Zum Biegeschubversagen schlanker Bauteile aus Hochleistungsbeton mit und ohne Vorspannung*, Dissertation, Universität Leipzig, 2000.
- [12] Hillerborg, A. “Analysis of one Single Crack”, *Fracture Mechanics of Concrete*, 1983.
- [13] Model Code *Model Code 2010 – First complete draft, Volume 1*, Lausanne: International Federation for Structural Concrete (fib), 2010.
- [14] Rimmel, G., “Zum Zug- und Schubtragverhalten von Bauteilen aus hochfestem Beton”, *DAfStb-Heft 444*, 1994.
- [15] Grimm, R., “Einfluß bruchmechanischer Kenngrößen auf das Biege- und Schubtragverhalten hochfester Betone”, *DAfStb-Heft 447*, 1997.
- [16] Reinhardt, H.-W., Cornelissen, H., Hordijk, D.A., “Tensile Tests and failure Analysis of Concrete”, *Journal of Structural Engineering*, 112(11), 2462-2477, 1986.
- [17] Baumann, T., Rüsck, H., “Versuche zum Studium der Verdübelungswirkung der Biegezugbewehrung eines Stahlbetonbalkens” *DAfStb-Heft 210*, 1970.
- [18] prEN 1994-1-1, *Eurocode 4: Design of composite steel and concrete structures – Part 1-1: General rules and rules for buildings – SC4.T6: Draft prEN 1994-1-1:042020 + comments*. CEN European Committee for Standardization.
- [19] Schmeckebeier, N. *Ein Ingenieurmodell zur Berechnung der Querkrafttragfähigkeit von Stahlverbunddecken des Hochbaus mit praxisrelevanter Betonstahlbewehrung*, Dissertation, Technische Universität Kaiserslautern, 2021.

EUROPEAN CODE DEVELOPMENTS

Stephen J. Hicks*, **Markus Schäfer****, **Graham Couchman*****

* School of Engineering, University of Warwick, Coventry, UK (Vice-chair of CEN/TC250/SC4 and member of project team CEN/TC250/SC4.T3, SC4.T5 and SC4.T6)

e-mail: Stephen.J.Hicks@warwick.ac.uk

** University of Luxembourg, Department of Engineering, Structural Engineering & Composite Structures (Convener of CEN/TC250/SC4.T6 and member of project team CEN/TC250/SC4.T1)

e-mail: markus.schaefer@uni.lu

*** SCI, Ascot, UK (Chair of CEN/TC250/SC4)

e-mail: G.Couchman@steel-sci.com

Keywords: Eurocode 4, Second generation of Eurocode 4, Codes and Standards, Composite.

Abstract *The second generation of Eurocode 4 has been developed through several project teams that report to CEN TC250 Subcommittee 4 (CEN/TC250/SC4) ‘Design of composite steel and concrete structures’, which is chaired by Dr Graham Couchman. Given that work on the revised version of Eurocode 4 is nearing completion, this paper presents a selection of the changes that will be included, together with some of the technical challenges that needed to be overcome. Finally, further enhancements that might be considered worthy for inclusion within future editions of this standard are presented.*

1 INTRODUCTION

Work on the Eurocodes commenced in 1975 when the European Commission decided on ‘an action programme in the field of construction’ based on article 95 of the Treaty of Rome, which was aimed at ‘the elimination of technical obstacles to trade and harmonisation of technical specifications’. The Commission of European Communities (CEC) published eight European codes, or ‘Eurocodes’, for the design and execution of buildings and civil engineering structures. From these eight documents, the code for composite steel and concrete structures was published as Eurocode No. 4 in 1985 [1], which was based on the: ECCS Model Code [2]; international studies; together with Eurocode No. 1 (Common unified rules for different types of construction and material), No. 2 (Common unified rules for concrete structures), and No. 3 (Common unified rules for steel structures). The European Commission transferred the preparation and the publication of the Eurocodes to the European Committee for Standardization (CEN) in 1989 through a series of mandates, in order to provide them with the status of a European Standard (EN). In the same year, the Construction Products Directive (CPD), was issued which introduced the concept of CE Marking for all construction products permanently incorporated into construction works [3].

Under the direction of Technical Committee CEN/TC250, the Eurocodes were published by CEN in 1992 as European pre-standards (ENV). Due to difficulties in harmonizing all aspects, the ENV Eurocodes included “boxed values” which permitted Member States to choose values for use within their territory through the publication of National Application Documents (NADs). Subcommittee 4 (CEN/TC250/SC4) was responsible for the ENV Eurocode 4, which was published in three Parts *viz.* ENV 1994-1-1 [4], ENV 1994-1-2 [5], and ENV 1994-2 [6]. To avoid repetition of information, and reduce potential ambiguity, values and properties are only given in one Eurocode. Because of this, ENV Eurocode 4 provided extensive cross-referencing to the ENV Eurocode 2 and Eurocode 3.

The EU mandate to CEN required that the content of the final ENs should be limited to the ENV versions modified in response to national comments; this became challenging in the development of the EN

Eurocode 4 due to changes in Eurocode 2 and Eurocode 3 that had been made to address these comments which, *inter alia*, included increasing the maximum yield strength of structural steel from 355 MPa to 460 MPa. Moreover, from national comments relating to the ease of use of ENV 1994-2 for bridge designers, the Eurocode 4 project team were given permission to repeat the ‘general’ Part 1-1 rules within Part 2 [7]. For the design of composite steel and concrete structures, the EN Eurocode 4 was published in the following three parts:

- EN 1994-1-1, Part 1-1: General rules and rules for buildings [8].
- EN 1994-1-2, Part 1-2: General rules – Structural fire design [9].
- EN 1994-2, Part 2: General rules and rules for bridges [10].

To enable the EN Eurocodes to be used within a particular territory, National Standards Bodies (NSBs) have published National Annexes (NAs) which contain: Nationally Determined Parameters (NDPs) (values of partial safety factors and classes applicable to that country, country specific data, and values where only a symbol is given in the EN); decisions on the status of informative annexes; and references to non-contradictory complementary information (NCCI). After a coexistence period, the EN Eurocodes replaced the former national standards in 2010 in countries that are members of CEN. The Construction Products Regulation (CPR) [11] replaced the CPD in 2011, which resulted in CE Marking becoming mandatory from 1st July 2013. The above provides a brief overview of the history of Eurocode 4 up to the EN version; a much more comprehensive review of the development from 1970 to 2010 is presented by Johnson [7]. More recently, the Eurocodes were adopted as national standards in Singapore [12], and it is anticipated that other countries may soon be implementing them, such as Hong Kong, Macau, Malaysia, Vietnam, Sri Lanka and Indonesia [13].

Following the publication of Mandate M/515 by the European Commission [14], work on the second generation of the Eurocodes commenced in 2015. Given that the work programme is nearing completion, the revised version of Eurocode 4 will soon become available. This paper presents a selection of the changes that will be included within the second generation of Eurocode 4, Part 1-1 (hereafter referred to as prEN 1994-1-1) [15], as well as highlighting future areas of improvement which may be considered worthy for future revisions.

2 SECOND GENERATION OF EUROCODE 4

A response to Mandate M/515 was prepared by CEN/TC250 [16], which set-out an ambitious and detailed work programme where discrete tasks are undertaken under the direction of one of TC250’s existing subcommittees, working groups or horizontal groups. The mandate, *inter alia*, requires: extension of the Eurocodes in terms of new materials, products and construction methods; reduction in the number of NDPs (thereby leading to an alignment of safety levels); enhancing ‘ease of use’ for users; adoption of relevant ISO standards to supplement the Eurocodes (which implicitly recognizes the CEN-ISO Vienna agreement); and incorporation of recent results from scientific and technical associations, together with new research results. The revision can be broadly divided into two activities:

- General revisions and maintenance of the Eurocodes following the receipt of comments from the industry through a “systematic review” undertaken by NSBs.
- Technical enhancements of the Eurocodes within the scope of Mandate M/515.

For cases where there was insufficient agreement to develop a new EN, European Technical Specifications (CEN/TS) are also under development, which will complement and enlarge the suite of Eurocodes. A graphical representation of the structure for the second generation of the Eurocodes is presented in Figure 1.

The CEN/TC 250 work programme has been split into four overlapping phases, as follows:

- Phase 1: 25 Tasks (125 technical experts), 2015-2018
- Phase 2: 22 Tasks (88 technical experts), 2017-2020
- Phase 3 & 4: 26 Tasks (104 technical experts) 2018-2022

Each Task is the responsibility of a Project Team, which consists of a maximum of five or six members. The project team members were selected through a competitive tender and are contracted to the Royal
